



Contents lists available at ScienceDirect

European Journal of Mechanics B/Fluids

journal homepage: [www.elsevier.com/locate/ejmflu](http://www.elsevier.com/locate/ejmflu)

# The competing effects of wall transpiration and stretching on Homann stagnation-point flow

P.D. Weidman<sup>a,\*</sup>, Yi Ping Ma<sup>b</sup>

<sup>a</sup> Department of Mechanical Engineering, University of Colorado, Boulder, CO 80309, United States

<sup>b</sup> Department of Applied Mathematics, University of Colorado, Boulder, CO 80309, United States

## ARTICLE INFO

### Article history:

Available online xxx

### Keywords:

Homann stagnation-point flow  
Transpiration  
Radial stretching  
Nonuniqueness  
Stability

## ABSTRACT

The simultaneous effects of normal transpiration through a radially stretching porous plate beneath Homann stagnation-point flow are considered. The exact similarity reduction of the Navier–Stokes equations depends on the stretching parameter  $\lambda$  and the transpiration parameter  $\mu$ . Dual solutions are found over a limited range  $\lambda_c < \lambda < -1$  in the case of suction ( $\mu > 0$ ) but unique solutions exist for blowing ( $\mu < 0$ ). It is shown that the range of dual solutions increases with  $\mu$ , but a self-similar stability analysis reveals that the lower solution branches are unstable while upper solution branches are stable.

© 2016 Elsevier Masson SAS. All rights reserved.

## 1. Introduction

Many problems have addressed two-dimensional stagnation-point flow with a stretching boundary and/or a porous boundary with suction and/or blowing, sometimes for nanofluids and sometimes with an imposed magnetic field. Here we review relevant publications for axisymmetric Homann [1] stagnation-point flow for various plate boundary conditions. Wang [2] studied axisymmetric stagnation flow towards a moving plate. Weidman and Mahalingham [3] reported on the problem of Homann stagnation-point flow impinging on a transversely oscillating plate with suction. Attia [4] studied Homann hydromagnetic flow and heat transfer with uniform suction and injection. Velocity profiles were given for suction and injection in the absence of a magnetic field. Mahapatra and Gupta [5] reported on Homann stagnation-point flow impinging on a radially stretching surface. They find that a regular boundary-layer structure appears when the stretching velocity is less than the free stream velocity and that otherwise an inverted boundary layer is formed. Wang [6] reported, *inter alia*, on Homann stagnation flow directed towards a shrinking sheet. Attia [7] studied Homann hydromagnetic point flow impinging on a radially stretching sheet with heat generation in which results were given in the absence of a magnetic field. No publica-

tions were found that included both radial stretching of, and transpiration through, the surface bounding Homann stagnation-point flow.

The focus of the present endeavor is twofold. First we consider the simultaneous effects of transpiration, characterized by parameter  $\mu$ , and plate stretching, characterized by parameter  $\lambda$ , on the self-similar reduction of the Navier–Stokes equations. Second, the linear temporal stability of both the unique and dual solutions is determined.

The presentation proceeds as follows. In Section 2 the boundary-value problem for Homann [1] stagnation-point flow impinging on a porous stretching/shrinking plate with suction/blowing is formulated and solved numerically. An analysis of behavior near the right focal point is given in Section 2.1 and that near the left focal point is given in Section 2.2. The large  $\mu$  and large  $\lambda$  asymptotic behaviors are given in Section 2.3 and Section 2.4, respectively. The stability of the unique and dual solutions encountered is determined following the method of Merkin [8] in Section 3. A discussion of results and concluding remarks are given in Section 4.

## 2. Formulation and solution

Consider axisymmetric Homann stagnation point flow for which  $(r, z)$  are the radial and axial coordinates with corresponding velocities  $(u, w)$ . For flow above a flat porous disk, the unsteady continuity and Navier–Stokes equations for an

\* Corresponding author.

E-mail address: [weidman@colorado.edu](mailto:weidman@colorado.edu) (P.D. Weidman).

incompressible fluid are

$$\frac{1}{r} \frac{\partial(ru)}{\partial r} + \frac{\partial w}{\partial z} = 0 \tag{1a}$$

$$\frac{\partial u}{\partial t} + u \frac{\partial u}{\partial r} + w \frac{\partial u}{\partial z} = -\frac{\partial p}{\partial r} + \nu \left( \frac{\partial^2 u}{\partial r^2} + \frac{1}{r} \frac{\partial u}{\partial r} + \frac{\partial^2 u}{\partial z^2} - \frac{u}{r^2} \right) \tag{1b}$$

$$\frac{\partial w}{\partial t} + u \frac{\partial w}{\partial r} + w \frac{\partial w}{\partial z} = -\frac{\partial p}{\partial z} + \nu \left( \frac{\partial^2 w}{\partial r^2} + \frac{1}{r} \frac{\partial w}{\partial r} + \frac{\partial^2 w}{\partial z^2} \right) \tag{1c}$$

wherein  $\rho$  is the fluid density and  $\nu$  is the kinematic viscosity, both assumed constant, and  $p$  is the pressure. We adopt the unsteady similarity transformation

$$u(r, z) = arf'(\eta), \quad w(r, z) = -2\sqrt{av}f(\eta), \tag{2}$$

$$\eta = \sqrt{\frac{a}{\nu}} z, \quad \tau = at$$

where  $a$  is the strain rate of the stagnation-point flow. Setting  $f'(0) = \lambda$  gives linear radial stretching for  $\lambda > 0$  and linear radial shrinking for  $\lambda < 0$ . Setting  $f(0) = \mu$  gives uniform suction for  $\mu > 0$  and uniform blowing for  $\mu < 0$ . The ansatz (2) satisfies the continuity equation (1a) and substitution into the unsteady Navier–Stokes equations (1b) and (1c) gives

$$f''' + 2ff'' - f'^2 + 1 - f'_\tau = 0 \tag{3a}$$

$$f(0) = \mu, \tag{3b}$$

$$f'(0) = \lambda, \tag{3c}$$

$$f'(\infty) = 1. \tag{3d}$$

The compatible steady flow pressure field is

$$p(r, \eta) = p_0 - \rho \left[ \frac{a^2 r^2}{2} + 2av(f^2 + f') \right] \tag{4a}$$

where  $p_0$  is the pressure at  $r = \eta = 0$ , namely

$$p_0 = 2\rho av(\mu^2 + \lambda). \tag{4b}$$

Solutions of the steady flow problem for  $f''(0)$ , at each value of  $\mu$  and  $\lambda$ , are related to the radial wall shear stress  $\tau$  through the expression

$$\tau = \mu \frac{\partial u}{\partial z} \Big|_{z=0} = \rho v^{1/2} a^{3/2} r f''(0) \tag{5}$$

showing that the shear stress increases linearly with radius.

We denote focal points in  $\lambda$ - $f''(0)$  space using  $\{\lambda, f''(0)\}$ . The obvious exact solution  $f(\eta) = \eta$ , valid for all transpirations  $\mu$ , exists at the  $\{1, 0\}$  focal point of the system. Solutions for  $\mu = 0$  are those analyzed previously by Wang [6]. Numerical integrations carried out for  $\mu = -0.5, -0.25, 0.0, 0.25$  and  $0.5$  are displayed in  $\lambda$ - $f''(0)$  parameter space in Fig. 1. Integrations carried out using a standard shooting method incurred difficulties at various negative values of  $\lambda$ . The integration method ODEINT found in Press, et al. [9], has been used with great success on a number of problems, but in certain instances the shooting iteration becomes difficult as more and more precise values of  $f''(0)$  are needed to obtain a converged solution. As a result, integrations were completed using the continuation code AUTO; see Doedel [10].

The results for suction ( $\mu > 0$ ) in Fig. 1 exhibit features similar to those found in the boundary-layer flows studied by Weidman, et al. [11,12] and Bhattacharyya and Layet [13]: there is a region

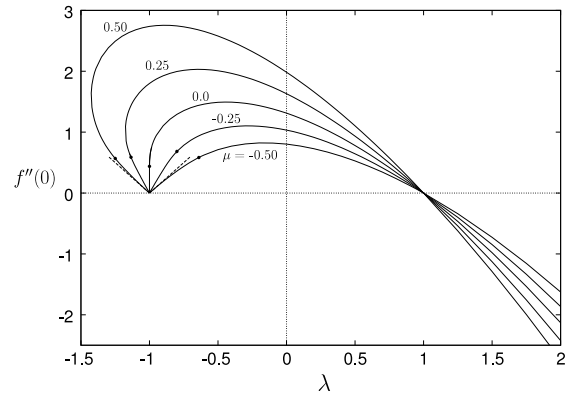


Fig. 1. Parametric solution curves of  $f''(0)$  as a function of  $\lambda$  for selected values of  $\mu$  indicated. The dots show the demarcation between curves computed using a FORTRAN shooting code and the final approach to the focal point at  $\lambda = -1$  using AUTO. The dashed lines are the slope of the curves given by Eq. (13) at the left focal point for  $\mu = -0.5$  and  $0.5$ .

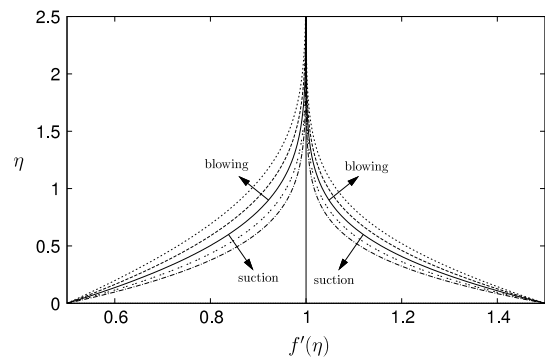


Fig. 2. Velocity profiles for  $\lambda = 0.5$  and  $\lambda = 1.5$  showing the effects of suction and blowing about the zero transpiration profile marked as a solid line. The values of  $\mu$  are  $\{-0.50, -0.25, 0.0, 0.25, 0.50\}$ .

Table 1  
Variation of  $\lambda_c$  with transpiration parameter  $\mu$ .

$\mu$	$\lambda_c$
0.50	-1.425
0.25	-1.175
0.00	-1.0

of unique solutions for  $\lambda > -1$ , dual solutions for  $\lambda_c < \lambda \leq -1$  and no solutions for  $\lambda < \lambda_c$ . The critical values of  $\lambda_c$  accurate to four decimal places are provided in Table 1. For blowing ( $\mu < 0$ ), on the other hand, solutions are unique for all  $\lambda > -1$ .

Sample similarity velocity profiles  $f'(\eta)$  presented in Fig. 2 quantify the effect of suction and blowing at positive  $\lambda$ . The results for  $\lambda = 0.5$  corresponding to a disk stretching from the origin at half the speed of the free stream and those plotted for  $\lambda = 1.5$  correspond to a disk stretching 50% faster than the free stream. In both cases suction increases the skin friction measured by  $f''(0)$  and decreases the boundary layer thickness, while the opposite is true for blowing.

For negative values of  $\lambda$  the profiles along the curve  $\mu = 0.5$  have unique solutions in the range  $-1 \leq \lambda \leq 0$  and dual solutions in the range  $-1.425 < \lambda \leq -1.0$ . Velocity profiles along this curve are displayed in Fig. 3(a). For  $\mu = -0.5$  there are only unique solutions for all  $\lambda \geq -1$ . Sample velocity profiles for  $\mu = -0.5$  at selected values of  $\lambda$  are shown in Fig. 3(b).

Note that, in addition to the focal point at  $\{1, 0\}$ , there is another zero stress focal point at  $\{-1, 0\}$ . Analysis of solutions near these points helps to elucidate local solution behaviors. We consider

Download English Version:

<https://daneshyari.com/en/article/7051178>

Download Persian Version:

<https://daneshyari.com/article/7051178>

[Daneshyari.com](https://daneshyari.com)